

# Journal of Materials Chemistry C

Materials for optical, magnetic and electronic devices

[www.rsc.org/MaterialsC](http://www.rsc.org/MaterialsC)



Themed issue: Spin-state Switches in Molecular Materials Chemistry

ISSN 2050-7526



COMMUNICATION

Keita Kuroiwa *et al.*

Supramolecular control of reverse spin transitions in cobalt(II) terpyridine complexes with diblock copolypeptide amphiphiles

Cite this: *J. Mater. Chem. C*, 2015,  
3, 7779Received 10th March 2015,  
Accepted 24th March 2015

DOI: 10.1039/c5tc00677e

www.rsc.org/MaterialsC

Supramolecular control of reverse spin transitions  
in cobalt(II) terpyridine complexes with diblock  
copolypeptide amphiphiles†Keita Kuroiwa,<sup>a</sup> Tsubasa Arie,<sup>a</sup> Shinichi Sakurai,<sup>b</sup> Shinya Hayami<sup>c</sup> and  
Timothy J. Deming<sup>d</sup>

Three composites composed of the cobalt terpyridine complex [Co<sup>II</sup>(MeO-terpy)<sub>2</sub>] and the diblock copolypeptide amphiphiles **1** and **2** or the polypeptide **3** (including glutamic acid and leucine) were prepared. Supramolecular structures such as rectangular morphologies were obtained from composites of **1** and **2**. A perfectly reversible reverse spin transition was successfully generated in the case of composites made with **1**.

Since spin crossover (SCO) was first described by Cambi *et al.* in the 1930s, a number of compounds exhibiting this phenomenon have been reported.<sup>1–5</sup> The most significant developments in the field have occurred only in the past ten years, and have included the fabrication of films,<sup>6,7</sup> nanofibers<sup>8</sup> and gels,<sup>9,10</sup> that have been widely researched with the aim of developing magnetic and information storage devices. In addition, nanocomposites incorporating organic compounds such as surfactants,<sup>10</sup> liquid crystals<sup>11,12</sup> and polymers<sup>13,14</sup> have been created in which the spin information of a metal complex is propagated to the nanostructure, thus transmitting changes in spin-state throughout a material. The characteristics of nanocomposites incorporating a metal complex in contact with adjacent molecules within a highly-ordered structure are known to vary based on intermolecular interactions and packing, implying that enhanced spin crossover cooperativity is a consequence of long-range interactions between metal ions.

The SCO characteristics of cobalt(II) compounds also exhibit a 1/2 ⇌ 3/2 spin change. It is well-known that the discrete cobalt(II) compounds [Co(terpy)<sub>2</sub>]X<sub>2</sub>·nH<sub>2</sub>O (terpy = 2,2':6',2''-terpyridine,

X = halide, pseudohalide, BF<sub>4</sub><sup>−</sup>, NO<sub>3</sub><sup>−</sup> or ClO<sub>4</sub><sup>−</sup> and n = 0 to 5) have demonstrated gradual SCO behaviour.<sup>15</sup> Recently, the high molecular weight alkylated cobalt(II) compounds [Co(R-terpy)<sub>2</sub>](BF<sub>4</sub>)<sub>2</sub> (R-terpy = 4'-alkoxy-2,2':6',2''-terpyridine) have been reported to display a “reverse spin transition” between high-spin (HS) and low-spin (LS) states with a thermal hysteresis loop triggered by a structural phase transition.<sup>16,17</sup> It has been suggested that the flexibility of the alkyl chain plays an important role in the unique magnetic properties, intermolecular interactions and crystal properties of this compound. Ideally, the characteristics of such systems would be tuneable by controlling the spatial arrangement of the SCO metal complexes, resulting in intermolecular interaction among the metal complexes using supramolecules without covalent or coordinative linkages.

At present, the main focus is on the use of amphiphilic compounds as a means of developing supramolecular composites with metal complexes that will function as flexible nanostructural materials.<sup>18,19</sup> In particular, metalloproteins and enzymes containing flexible internal portions based on apoproteins may be obtained from the complex amino acids and metal centers found in biological systems.<sup>20</sup> Therefore, the presence of a flexible region is a key factor in the operation of functional metal complexes.

In our previous research, we developed an alternative approach to the design of metal complexes by compounding diblock copolypeptide amphiphiles, resulting in metal–metal interactions that generated photoluminescence in water.<sup>21</sup> Various diblock copolypeptide amphiphiles with metal cyanide complexes were found to exhibit unique morphologies, such as the formation of an elliptical shape with a woven pattern based on the alignment of the metal complexes. This technique of combining amphiphilic molecules with discrete coordination compounds makes it possible to design flexible, reversible and signal-responsive supramolecular coordination systems.

In the present study, we initially focussed on combining cobalt(II) terpyridine complexes with diblock copolypeptide amphiphiles and examining the SCO characteristics of the resulting complexes in water. We further investigated novel concepts designed to allow supramolecular control of the spin

<sup>a</sup> Department of Nanoscience, Faculty of Engineering, Sojo University, 4-22-1 Ikeda, Nishi-ku, Kumamoto 860-0082, Japan. E-mail: keitak@nano.sojo-u.ac.jp

<sup>b</sup> Department of Biobased Materials Science, Kyoto Institute of Technology, Matsugasaki, Sakyo-ku, Kyoto 606-8585, Japan

<sup>c</sup> Department of Chemistry, Graduate School of Science and Technology, Kumamoto University, 2-39-1 Kurokami, Chuo-ku, Kumamoto 860-8555, Japan

<sup>d</sup> Department of Bioengineering, University of California, Los Angeles, CA 90095, USA

† Electronic supplementary information (ESI) available: General information on materials and measurement, and SWAXS data. See DOI: 10.1039/c5tc00677e



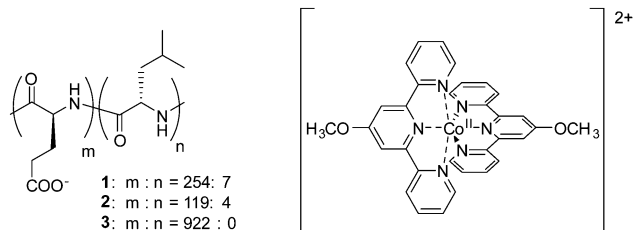


Fig. 1 Chemical structures of diblock copolypeptide amphiphiles **1** and **2**, the polypeptide **3** and the cobalt(II) terpyridine complex  $[\text{Co}^{\text{II}}(\text{MeO-terpy})_2]^{2+}$ .

state and to induce the reverse spin transition phenomenon through self-assembly, with the result that these complexes exhibited SCO with thermal hysteresis. The characteristics of this specific SCO, including the associated structural changes and complex morphologies, were elucidated by spectroscopic and microscopic analyses.

The diblock copolypeptide amphiphiles **1** and **2** and the polypeptide **3** (Fig. 1) were synthesized by modifying methods previously published in the literature (see ESI†).<sup>22</sup> Both **1** and **2** were synthesized so as to have a suitable degree of polymerization, since this is known to enhance the solubility of these compounds in water and also enhances the packing of the polypeptides in supramolecular assemblies, resulting in the formation of hydrogels.<sup>22</sup> In contrast, polymer **3** was synthesized to a higher degree of polymerization since it was not intended to produce a supramolecular effect. The cobalt(II) terpyridine complex containing the 4-methoxy-2,2':6',2''-terpyridine ligand was obtained by a method previously described in the literature.<sup>17</sup> Composites of polypeptides **1**–**3** and the cobalt(II) terpyridine complex were synthesized by mixing solutions of the respective compounds, followed by precipitation of the resulting composites, and by replacing the counteranion of  $[\text{Co}(\text{MeO-terpy})_2]^{2+}$  (see ESI†). Finally,  $1/[\text{Co}^{\text{II}}(\text{MeO-terpy})_2]$ ,  $2/[\text{Co}^{\text{II}}(\text{MeO-terpy})_2]$  and  $3/[\text{Co}^{\text{II}}(\text{MeO-terpy})_2]$  were obtained by lyophilisation. Evaluation by elemental analysis indicated the presence of water molecules in the final products ( $1/[\text{Co}^{\text{II}}(\text{MeO-terpy})_2] \cdot \text{H}_2\text{O}$ ,  $2/[\text{Co}^{\text{II}}(\text{MeO-terpy})_2] \cdot 3\text{H}_2\text{O}$  and  $3/[\text{Co}^{\text{II}}(\text{MeO-terpy})_2] \cdot 4\text{H}_2\text{O}$ ).

When  $1/[\text{Co}^{\text{II}}(\text{MeO-terpy})_2]$  was dissolved in room temperature water at a concentration of 5 mM (on the basis of  $\text{Co}^{\text{II}}$  ions), a pale-purple, cloudy dispersion was obtained. This result indicated both the inclusion of the metal complex and the formation of a homogeneous, colloidal dispersion of the complex in the solvent. The  $2/[\text{Co}^{\text{II}}(\text{MeO-terpy})_2]$  composite also dissolved in water to give a pale-purple, cloudy solution, whereas  $3/[\text{Co}^{\text{II}}(\text{MeO-terpy})_2]$  gave a transparent solution, indicating that this composite was dispersed on the molecular level.

Transmission electron microscopy (TEM) was used to determine the morphology of the supramolecular structures generated by these complexes in the cloudy dispersions. Fig. 2 shows a TEM image of  $1/[\text{Co}^{\text{II}}(\text{MeO-terpy})_2]$  following transfer to a carbon-coated Cu grid, in which rectangular structures with widths of 700 nm to 6  $\mu\text{m}$  are evident (Fig. 2a). A similar analysis of  $2/[\text{Co}^{\text{II}}(\text{MeO-terpy})_2]$  showed that the widths of the resulting nanostructures ranged from 500 nm to 2  $\mu\text{m}$  (Fig. 2b). Using the Corey–Pauling–Kultun (CPK) model, the polypeptide lengths in **1** and **2** were estimated to

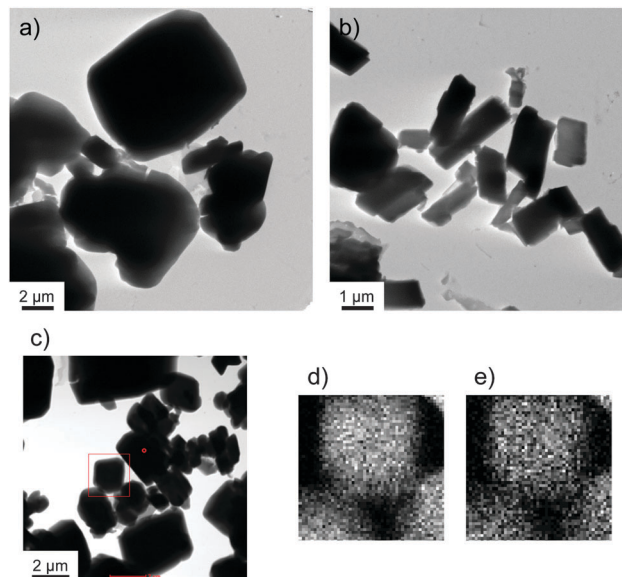


Fig. 2 HR-TEM images of (a)  $1/[\text{Co}^{\text{II}}(\text{MeO-terpy})_2]$  and (b)  $2/[\text{Co}^{\text{II}}(\text{MeO-terpy})_2]$  samples as prepared from water dispersions. (c) STEM image and (d) Co and (e) O STEM-EDX maps of  $1/[\text{Co}^{\text{II}}(\text{MeO-terpy})_2]$  within the red square shown in (c).

be in the range of 900–1900 Å (**1**, *ca.* 1900 Å; **2**, *ca.* 900 Å), hence the rectangular structure seen in the TEM images being more than ten times the length of the diblock copolypeptide amphiphiles. These structures are therefore composed of multiple strands of linear and/or stacked polypeptides combined with the metal complex.

High resolution scanning transmission electron microscopy coupled with energy dispersive X-ray spectroscopy (HR-STEM EDX) also confirmed that the composites consisted of cobalt(II) complexes and polymers. Fig. 2d and e present the STEM EDX mapping (Fig. 2d, Co; Fig. 2e, O) of nanocomposites of **1** within the boxed area indicated in Fig. 2c. These data confirm the formation of nanostructures in which the cobalt complex and the amphiphile are evenly matched. Composite  $3/[\text{Co}^{\text{II}}(\text{MeO-terpy})_2]$  did not show a specific structure in TEM observations, indicating that combinations of **3** and metal complexes do not form a supramolecular structure.

The size distributions of the nanostructures in water were also analysed by dynamic light scattering (DLS). DLS data obtained for  $1/[\text{Co}^{\text{II}}(\text{MeO-terpy})_2]$  and  $2/[\text{Co}^{\text{II}}(\text{MeO-terpy})_2]$  at 293 K indicated at least three peaks in the volume-based mean nanostructure size distributions, at approximately 200 nm, 1  $\mu\text{m}$  and 40  $\mu\text{m}$  (Fig. 3). These results are consistent with the rectangular nanostructures having widths of several hundred nm and several  $\mu\text{m}$  observed in the TEM images, although DLS can only evaluate the hydrodynamic radii of dispersed structures in a solvent. In contrast,  $3/[\text{Co}^{\text{II}}(\text{MeO-terpy})_2]$  did not generate a light scattering signal. The results demonstrate that the use of diblock copolypeptide amphiphiles led to supramolecular structures in water.

Samples of the composites in water were freeze-dried and wide angle X-ray scattering (WAXS) analysis of the powdered composites was performed (Fig. S1a, ESI†), which did not generate





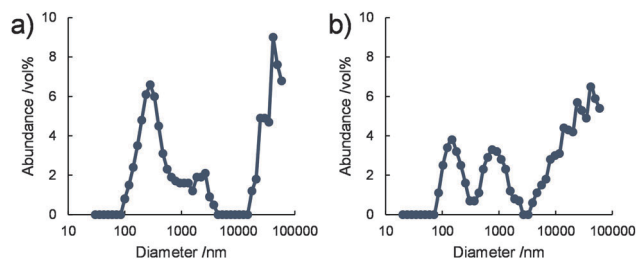


Fig. 3 Volume-based size distributions obtained by DLS for (a)  $1/[\text{Co}^{\text{II}}(\text{MeO-terpy})_2]$  and (b)  $2/[\text{Co}^{\text{II}}(\text{MeO-terpy})_2]$  in water at 293 K.  $[\text{Co}] = 5 \text{ mM}$ .

any crystalline peaks in WAXS. This lack of peaks indicates the presence of an amorphous phase in the rectangular supra-molecular structures. In addition, small angle X-ray scattering (SAXS) analysis (Fig. S1b, ESI<sup>†</sup>) indicates the formation of nanostructures in a various sizes, which are consistent with the nanostructures with widths of several hundred nm and several  $\mu\text{m}$  observed in the TEM and DLS.

The variations in the magnetic susceptibilities of  $1/[\text{Co}^{\text{II}}(\text{MeO-terpy})_2]$ ,  $2/[\text{Co}^{\text{II}}(\text{MeO-terpy})_2]$  and  $3/[\text{Co}^{\text{II}}(\text{MeO-terpy})_2]$  with temperature were examined. Composite  $1/[\text{Co}^{\text{II}}(\text{MeO-terpy})_2]$  was found to exist in the HS state at all temperatures and exhibited a  $\chi_{\text{m}}T$  value within the range of  $1.69\text{--}2.25 \text{ cm}^3 \text{ K mol}^{-1}$  over the temperature range of  $5\text{--}300 \text{ K}$  (the blue plot in Fig. 4a). On further heating to  $400 \text{ K}$ , the  $\chi_{\text{m}}T$  value was found to decrease at  $337 \text{ K}$ , consistent with the loss of water molecules (the red plot in Fig. 4a).

However, after annealing, the pre-heated compound displayed markedly different behaviour. The  $\chi_{\text{m}}T$  value gradually decreased from  $1.60 \text{ cm}^3 \text{ K mol}^{-1}$  at  $400 \text{ K}$  to  $1.05 \text{ cm}^3 \text{ K mol}^{-1}$  at  $274 \text{ K}$ , representing normal thermal SCO behaviour (red plot in Fig. 4a). Upon further cooling, the  $\chi_{\text{m}}T$  value increased abruptly below  $T_{1/2} \downarrow = 260 \text{ K}$ , to  $1.96$  at  $222 \text{ K}$ . On further cooling, the  $\chi_{\text{m}}T$

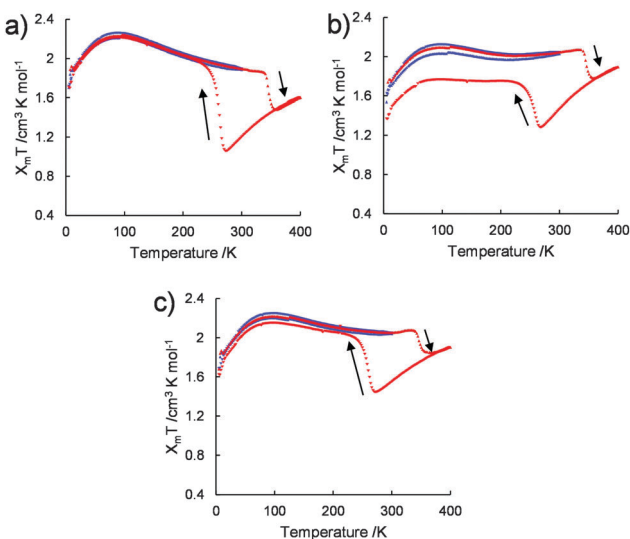


Fig. 4  $\chi_{\text{m}}T$  versus  $T$  for (a)  $1/[\text{Co}^{\text{II}}(\text{MeO-terpy})_2]$ , (b)  $2/[\text{Co}^{\text{II}}(\text{MeO-terpy})_2]$  and (c)  $3/[\text{Co}^{\text{II}}(\text{MeO-terpy})_2]$  on warming ( $\blacktriangle$ ) and cooling ( $\blacktriangledown$ ). The blue plots indicate the first cycle (from  $5$  to  $300 \text{ K}$ ) and the red plots indicate the second cycle above the boiling point of water (from  $5$  to  $400 \text{ K}$ ).

varied between  $1.70 \text{ cm}^3 \text{ K mol}^{-1}$  and  $2.20 \text{ cm}^3 \text{ K mol}^{-1}$  in the temperature range between  $5$  and  $220 \text{ K}$ . On further heating, the  $\chi_{\text{m}}T$  value abruptly dropped ( $T_{1/2} \uparrow = 345 \text{ K}$ ), showing the transition from HS to LS. Finally, the  $\chi_{\text{m}}T$  value gradually increased between  $361$  and  $400 \text{ K}$ . The wide thermal hysteresis loop ( $\Delta T = 85 \text{ K}$ ) near room temperature was maintained through successive thermal cycles.

Composites  $2/[\text{Co}^{\text{II}}(\text{MeO-terpy})_2]$  (Fig. 4b) and  $3/[\text{Co}^{\text{II}}(\text{MeO-terpy})_2]$  (Fig. 4c) also showed abnormal reverse spin transitions during heating and cooling cycles ( $5\text{--}300\text{--}5\text{--}400\text{--}5 \text{ K}$ ). Reversibility between the HS and LS states in the reverse spin transition, however, was dependent on the polymer employed. In particular, the diblock copolyptide amphiphile **1** evidently possessed a suitable degree of polymerization and a balance between hydrophilic and hydrophobic portions, leading to perfect reversibility between the HS and LS states to generate reverse spin transition. Thus reverse spin transition<sup>16</sup> was obtained from the composite in its solvated state based on intermolecular interactions among the metal complexes.

The  $[\text{Co}^{\text{II}}(\text{MeO-terpy})_2]^{2+}$  complex with  $\text{BF}_4^-$  anions is typically observed to undergo a gradual SCO with the transition centred around  $T_{1/2} = 100\text{--}300 \text{ K}$ .<sup>17</sup> During this process, water molecules in the solvent have been found to play an important role in the SCO behaviour, due to either two-step SCO ( $\text{H}_2\text{O}$ -solvated complex) or one-step SCO (non-solvated complex). In addition, reverse spin transition can be achieved using an organic-solvated metal complex in solvents such as acetone in association with a structural phase transition.<sup>17</sup> These prior results suggest that the SCO of the aqueous dispersions of solid composites of polymers and a cobalt(II) terpyridine complex should be accompanied by a transition between solvated and non-solvated phases since the metal complex is dispersed in the amphiphilic polypeptide-induced nanostructures.

Our morphological and magnetic investigations were able to provide details concerning the supra-molecular structure of the composites made with  $[\text{Co}^{\text{II}}(\text{MeO-terpy})_2]^{2+}$ , as illustrated in Fig. 5. The results of elemental analysis showed that the composites were composed of  $[\text{Co}^{\text{II}}(\text{MeO-terpy})_2]^{2+}$  and the hydrophilic peptide in a  $1:4$  ratio. In addition, since reversible transitions of the magnetic properties between solvated and non-solvated phases (Fig. 4) have been obtained when using a suitable diblock copolyptide amphiphile with a metal complex,<sup>21</sup> the metal complexes must be partially aligned to one another in the polypeptide composites. Indeed, supra-molecular structures on the sub-nanometre to micrometre scale were observed by DLS and TEM, indicating that the hydrophobic interactions of the leucine moiety (Fig. 5b) determine the  $\text{H}_2\text{O}$ -solvated and non-solvated forms of the composites, reversibly. Typically, 1D  $\text{Co}(\text{II})$  complexes in organic media have been found to be sensitive to solvation with water molecules.<sup>23</sup> Thus, one possible arrangement among metal complexes that can be proposed is moderate packing of 1D or 2D sheets (Fig. 5c). The close-packed structure of cobalt(II) terpyridine complexes exhibiting reverse spin transition as obtained from crystallographic data shows a two-dimensional array of metal complexes extending along the crystallographic  $bc$  plane, with minimal order, resulting in a



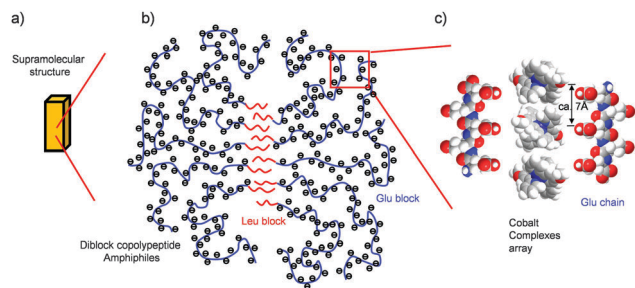


Fig. 5 Hierarchical schematic illustration of the self-assembly of diblock copolypeptide amphiphiles/[Co<sup>II</sup>(MeO-terpy)<sub>2</sub>], showing how a rectangular structure (a) is formed from diblock copolypeptide amphiphiles with cobalt(II) complexes (b, c).

loose packing arrangement.<sup>17</sup> In this structure, the cobalt(II) complexes are aligned with an average separation between nearest molecules of 6–7 Å, which is consistent with the distance between the neighbouring carboxylic acid units (ca. 0.7 nm, as estimated by the CPK model; Fig. 5c) when polyglutamic acid forms β sheet with an all-*trans* conformation, partially. Therefore, reversible reverse spin transition is thought to result from the balance between the amorphous diblock copolypeptide amphiphiles and the loose packing of the cobalt(II) terpyridine complexes.

## Conclusions

In conclusion, we have demonstrated that composites consisting of a cobalt(II) terpyridine complex with diblock copolypeptide amphiphiles generate supramolecular structures in water. The formation of these nanostructures results in the evolution of morphologies ranging in size from sub-nanometre to several micrometres. Moreover, these supramolecular composites display reverse spin transition depending on the polypeptide structures. Changes in both the morphology and magnetic properties of these materials can be induced by variations in the temperature and solvated phase. The technique of combining polypeptide molecules and discrete coordination compounds thus makes it possible to design flexible, reversible and spin-controllable supramolecular coordination systems. The concept of composites based on diblock copolypeptide amphiphiles could also be expanded to generate other useful coordination compounds and should allow us to further develop the nanochemistry of element-block composites.

## Acknowledgements

This work was financially supported in part by a Grant-in-Aid for Young Scientists (A) (No. 24685019) and a Grant-in-Aid for Scientific Research on Innovative Areas (New polymeric materials based on element-blocks, #2401) (No. 25102547).

## Notes and references

- 1 L. Cambi and L. Szego, *Ber. Dtsch. Chem. Ges. B*, 1931, **64**, 259.

- 2 P. Gütllich and H. A. Goodwin, *Spin Crossover in Transition Metal Compounds I – III*, Topics in Current Chemistry, Springer, Heidelberg, 2004, vol. 233–235 and reference therein.
- 3 O. Kahn and J. C. Martinez, *Science*, 1998, **279**, 44–48.
- 4 O. Kahn, *Acc. Chem. Res.*, 2000, **33**, 647–657.
- 5 O. Kahn, J. Kröber and C. Jay, *Adv. Mater.*, 1992, **4**, 718–728.
- 6 A. Nakamoto, Y. Ono, N. Kojima, D. Matsumura, T. Yokoyama, X. J. Liu and Y. Morimoto, *Synth. Met.*, 2003, **137**, 1219; A. Nakamoto, Y. Ono, N. Kojima, D. Matsumura and T. Yokoyama, *Chem. Lett.*, 2003, **32**, 336; A. Nakamoto, N. Kojima, L. XiaoJun, Y. Morimoto and A. Nakamura, *Polyhedron*, 2005, **24**, 2909.
- 7 F. Armand, C. Badoux, P. Bonville, A. Ruaudel-Teixier and O. Kahn, *Langmuir*, 1995, **11**, 3467–3472.
- 8 K. Kuroiwa and N. Kimizuka, *Polym. J.*, 2013, **45**, 3842; T. Shibata, N. Kimizuka and T. Kunitake, *The 76th CSJ National meeting*, 1999, 4F1 37; N. Kimizuka and T. Shibata, *Polym. Preprints Jpn.*, 2000, **49**(1S18), 3774.
- 9 K. Kuroiwa, T. Shibata, S. Sasaki, M. Ohba, A. Takahara, T. Kunitake and N. Kimizuka, *J. Polym. Sci., Part A: Polym. Chem.*, 2006, **44**, 5192; S. Kume, K. Kuroiwa and N. Kimizuka, *Chem. Commun.*, 2006, 2442; K. Kuroiwa and N. Kimizuka, *Chem. Lett.*, 2010, **39**, 790.
- 10 (a) O. Roubeau, A. Colin, V. Schmitt and R. Clérac, *Angew. Chem., Int. Ed.*, 2004, **43**, 3283; (b) T. Fujigaya, D.-L. Jiang and T. Aida, *Chem. – Asian J.*, 2007, **2**, 106.
- 11 E. Coronado, J. R. Galán-Mascarós, M. Monrabal-Capilla, J. García-Martínez and P. Pardo-Ibañez, *Adv. Mater.*, 2007, **19**, 1359.
- 12 K. Kuroiwa, H. Kikuchi and N. Kimizuka, *Chem. Commun.*, 2010, **46**, 1229.
- 13 A. B. Gaspar, V. Ksenofontov, M. Seredyuk and P. Gütllich, *Coord. Chem. Rev.*, 2005, **249**, 2661.
- 14 S.-W. Lee, J.-W. Lee, S.-H. Jeong, I.-W. Park, Y.-M. Kim and J.-I. Jin, *Synth. Met.*, 2004, **142**, 243; G. Schwarzanbacher, M. S. Gangl, M. Goriup, M. Winter, M. Grunert, F. Renz, W. Linert and R. Saf, *Monatsh. Chem.*, 2001, **132**, 519; R. Saf, G. Schwarzanbacher, C. Mirtl, G. Hayn, J. Hobisch and K. Gatterer, *Macromol. Rapid Commun.*, 2004, **25**, 911.
- 15 E. C. Constable, K. Harris, C. E. Housecroft, M. Neuburger and S. Schaffner, *Chem. Commun.*, 2008, 5360; E. C. Constable, K. Harris, C. E. Housecroft, M. Neuburger and J. A. Zampese, *Dalton Trans.*, 2011, **40**, 11441; J. Chambers, B. Eaves, D. Parker, R. Claxton, P. S. Ray and S. J. Slattery, *Inorg. Chim. Acta*, 2006, **359**, 2400.
- 16 S. Hayami, Y. Shigeyoshi, M. Akita, K. Inoue, K. Kato, K. Osaka, M. Takata, R. Kawajiri, T. Mitani and Y. Maeda, *Angew. Chem., Int. Ed.*, 2005, **44**, 4899; S. Hayami, R. Moriyama, A. Shuto, Y. Maeda, K. Ohta and K. Inoue, *Inorg. Chem.*, 2007, **46**, 7692; S. Hayami, K. Murata, D. Urakami, Y. Kojima, M. Akita and K. Inoue, *Chem. Commun.*, 2008, 6510; S. Hayami, K. Kato, Y. Komatsu, A. Fuyuhiko and M. Ohba, *Dalton Trans.*, 2011, **40**, 2167; Y. Komatsu, K. Kato, Y. Yamamoto, H. Kamihata, Y. H. Lee, F. Akita, S. Kawata and S. Hayami, *Eur. J. Inorg. Chem.*, 2012, 2769.



- 17 S. Hayami, M. Nakaya, H. Ohmagari, A. S. Alao, M. Nakamura, R. Ohtani, R. Yamaguchi, T. Kuroda-Sowa and J. K. Clegg, *Dalton Trans.*, 2015, DOI: 10.1039/C4DT03743J.
- 18 N. Kimizuka, *Adv. Polym. Sci.*, 2008, **219**, 1, and reference therein; H. Matsukizono, K. Kuroiwa and N. Kimizuka, *J. Am. Chem. Soc.*, 2008, **130**, 5622–5623.
- 19 K. Kuroiwa, M. Yoshida, S. Masaoka, K. Kaneko, K. Sakai and N. Kimizuka, *Angew. Chem., Int. Ed.*, 2012, **51**, 656.
- 20 Y. Mizutani and T. Kitagawa, *J. Phys. Chem. B*, 2001, **105**, 10992.
- 21 K. Kuroiwa, Y. Masaki, Y. Koga and T. J. Deming, *Int. J. Mol. Sci.*, 2013, **14**, 2022.
- 22 A. P. Nowak, V. Breedveld, L. Pakstis, B. Ozbas, D. J. Pine, D. Pochan and T. J. Deming, *Nature*, 2002, **417**, 424; C.-Y. Yang, B. Song, Y. Ao, A. P. Nowak, R. B. Abelowitz, R. A. Korsak, L. A. Havton, T. J. Deming and M. V. Sofroniew, *Biomaterials*, 2009, **30**, 2881.
- 23 K. Kuroiwa, T. Shibata, A. Takada, N. Nemoto and N. Kimizuka, *J. Am. Chem. Soc.*, 2004, **126**, 2016; K. Kuroiwa and N. Kimizuka, *Chem. Lett.*, 2008, **37**, 192.

